Research Square

Preprints are preliminary reports that have not undergone peer review.
They should not be considered conclusive, used to inform clinical practice,
or referenced by the media as validated information.

Comparative Evaluation of SNAP25 in Cerebrospinal Fluid and Plasma Across Three Cohorts

Mathias Sauer
University of Gothenburg
Luiza Santos Machado
University of Gothenburg
Charlotte Rocker
Fujirebio (Belgium)
Julie Goossens
Fujirebio (Belgium)
Lana Grötschel
University of Gothenburg
Shorena Janelidze
Lund University
Nesrine Rahmouni
McGill University
Federica Ribaldi
University of Geneva
Josepth Therriault
McGill University
Lydia Trudel
McGill University
Arthur C. Macedo
McGill University
Andréa Lessa Benedet
University of Gothenburg
Ann Brinkmalm
University of Gothenburg
Johan Gobom
University of Gothenburg
Michael Schöll
University of Gothenburg
Oskar Hansson
Lund University
Henrik Zetterberg
University of Gothenburg
Niklas Mattsson-Carlgren
Lund University
Pedro Rosa Neto
McGill University
Giovanni Frisoni
University of Geneva
Eugeen Vanmechelen
Fujirebio (Belgium)

Nicholas J. Ashton

nicholas.ashton@bannerhealth.com

University of Gothenburg

Research Article

Keywords: Alzheimer's disease, SNAP25, blood-based biomarkers, synaptic injury, SV2A PET, synaptic density, cerebrospinal fluid, synaptic dysfunction

Posted Date: November 6th, 2026

DOI: https://doi.org/10.21203/rs.3.rs-11320091/v1

License: This work is licensed under a Creative Commons Attribution 4.0 International License. Read Full License

Additional Declarations: Competing interest reported. HZ has served at scientific advisory boards and/or as a consultant for Abbvie, Acumen, Alamar, Alector, Alzinova, ALZpath, Amylyx, Annexon, Apellis, Artery Therapeutics, AZTherapies, Bioventix, Cognitact, Cognito Therapeutics, CogRx, Denali, Eisai, Enigma, Johnson & Johnson, LabCorp, Merck Sharp & Dohme, Merry Life, Nervgen, New Amsterdam, Novo Nordisk, Optoceutics, Passage Bio, Pinteon Therapeutics, Prothena, Quanterix, Red Abbey Labs, reMYND, Roche, Samumed, ScandiBio Therapeutics AB, Siemens Healthineers, Triplet Therapeutics, and Wave, has given lectures sponsored by Alzecure, BioArctic, Biogen, Cellectricon, Fujirebio, LabCorp, Lilly, Novo Nordisk, Oy Medix Biochemica AB, Roche, and WebMD, is a co-founder of Brain Biomarker Solutions in Gothenburg AB (BBS), which is a part of the GU Ventures Incubator Program, and is a shareholder of CERimmune Therapeutics (outside submitted work). OH is an employee of Eli Lilly. CDR, JG, and EV are employees of Fujirebio. All other authors report no conflicts of interest.

Abstract

Background

Synaptic dysfunction is a pathophysiological feature of Alzheimer's disease (AD). Although levels of synaptosomal-associated protein 25 (SNAP25) in cerebrospinal fluid (CSF) have been shown to be elevated, the utility of plasma SNAP25 and its relationship with synaptic density remains unclear. We evaluated and compared plasma and CSF SNAP25 across three independent cohorts, and examined associations with cognition and imaging outcomes, including synaptic vesicle glycoprotein 2A (SVA) positron emission tomography (PET).

Methods

SNAP25 was quantified by single-molecule array (SIMOA) in the BioFINDER-2 pilot (n = 102), Genova Memory Center (GMC; n = 106, plasma subset n = 42), and TRIAD (n = 36) cohorts. Participants were cognitively unimpaired (CU) or impaired (CI) and further stratified based on amyloid status (+/-). Group differences were tested adjusting for age, sex, and education, with Tukey corrections and diagnostic performance by ROC analyses and DeLong tests. Plasma-CSF effects were compared using mixed-effects models and Wald tests, and associations by Spearman/partial Spearman correlations and linear regressions. Plasma neurofilament light was used as an SV2A PET comparator.

Results

Plasma SNAP25 levels were elevated in CI+ across all cohorts (fold change = 1.46 in BioFINDER-2, 1.48 in GMC, and 1.77 in TRIAD, $p < 0.01$) compared to CU−, with AUCs of 0.78, 0.92, and 0.90 respectively. CSF group differences were less consistent, as were plasma-CSF correlations of SNAP25. Furthermore, in the BioFINDER-2, higher SNAP25 was associated with lower Mini-Mental State Examination scores, more brain atrophy, and greater amyloid and tau PET burden. Amyloid PET associations were also observed with CSF SNAP25 in GMC, and with plasma SNAP25 in TRIAD. In the full TRIAD cohort, plasma SNAP25 correlated with global SV2A PET meta-ROI after adjustment for age and sex (r_s=0.36, $p = 0.04$). In CI+ participants, there was also a significant association with global SV2A PET binding. Voxelwise plasma associations were strongest in the ventromedial prefrontal cortex. NfL was not associated with SV2A PET binding.

Conclusion

Plasma SNAP25 is reliably measurable and consistently elevated in CI+ individuals. Associations with core AD biomarkers and SV2A PET binding, particularly in CI+ individuals, support its potential as a marker of synaptic injury for disease characterisation and clinical-trial monitoring.

Background

Synaptic dysfunction and the loss of synaptic plasticity and integrity are distinct pathophysiological features in various forms of dementias such as Alzheimer's disease (AD), frontotemporal dementia (FTD), and dementia with Lewy bodies (DLB) [1–3]. It is also observed in other neurological and psychiatric disorders e.g., Parkinson's disease, amyotrophic lateral sclerosis, schizophrenia, and depression [2, 4–6]. Previous studies have found that synaptic degradation correlates strongly with cognitive decline in *e.g.*, AD, behavioural variant of FTD (bvFTD), and DLB [7–9]. The prevalence of synaptic degeneration in dementias, taken together with its strong correlation with cognitive decline presents a strong argument for implementing synaptic biomarkers into clinical routine for assessment of these neurodegenerative diseases to aid with diagnostics, predict disease progression, and stage disease severity. Robust synaptic biomarkers could also monitor the effects of drugs on synaptic health in clinical trials.

A strong candidate for the assessment of synaptic health is the presynaptic soluble N-ethylmaleimide-sensitive factor attachment receptor (SNARE) protein, synaptosomal-associated protein 25 (SNAP25). SNAP25 is essential for synaptic transmission and cognitive function due to its involvement in vesicular exocytosis, where it forms the SNARE complex together with vesicle-associated membrane proteins (VAMP) and syntaxin-1 [10]. Upon a Ca^{2+} influx of the synapse, the Ca^{2+} sensor protein synaptotagmin 1 binds the

calcium and interacts with the SNARE complex and phospholipids, thereby triggering a membrane fusion of the SNARE complex with the plasma membrane, enabling the release of neurotransmitters into the synaptic cleft [11, 12]. Several studies have shown that levels of SNAP25 in cerebrospinal fluid (CSF) is significantly higher in patients with both mild cognitive impairment (MCI) due to AD and dementia due to AD compared to cognitively unimpaired (CU) individuals [13–15]. Interestingly, CSF SNAP25 and other synaptic biomarkers such as neurogranin, growth-associated protein 43, and synaptotagmin-1 appear to be associated with amyloid pathology, as levels of these proteins have been shown to increase with amyloid burden [16, 17]. Consistent with these findings, several synaptic biomarkers do not show comparable elevations in non-AD neurodegenerative diseases, such as FTD, whereas increases are primarily observed in AD [18–20]. However, most studies of synaptic biomarkers in AD have focused on CSF, while blood-based studies remain comparatively limited.

Translation of synaptic biomarkers in CSF to blood has proven to be challenging, not only due to analytical sensitivity, but also because blood concentrations may reflect peripheral expression rather than CNS pathology. NPTX2 and neurogranin are two synaptic biomarkers where plasma levels do not mirror the AD-related changes seen in CSF [21–23]. Earlier blood-based synaptic biomarker studies therefore focused primarily on β-synuclein measured by immunoprecipitation–mass spectrometry [24]. Although targeted mass spectrometric methods can be analytically specific, their clinical implementation is limited by method-dependent performance, complex workflows, and throughput. More recently, there has been a fast development in ultrasensitive automated enzyme-linked immunosorbent assays (ELISA) that offers higher throughput, while retaining high analytical sensitivity [25]. Many synaptic proteins can now be measured on these platforms, such as SNAP25, neuronal pentraxin 2, and β-synuclein [23, 26, 27]. However, their biological and clinical validity as blood-based markers of synaptic dysfunction remains to be established [28, 29].

Another synaptic protein expressed throughout presynaptic terminals in the brain is synaptic vesicle glycoprotein 2 (SV2), which influences release of neurotransmitters by regulating the amount of synaptotagmin 1 in secretory vesicles [30]. There are three isoforms of SV2 (SV2A, SV2B, and SV2C), all of which are expressed in the brain, making the SV2 protein family a suitable marker for synaptic density [31–33]. Among these isoforms, SV2A is the only one expressed in synaptic vesicles across the whole brain, while the other two isoforms are expressed more sparingly, making SV2A the preferred biomarker for synaptic density [31, 32]. The preferred method to measure synaptic density through SV2A *in vivo* to date, is via positron emission tomography (PET) [34]. It has recently been reported that, in patients with AD, SV2A levels were significantly correlated with cognitive performance [35] and with fibrillary tau accumulation [36, 37].

In this study, we measured SNAP25 levels in both plasma and CSF across three independent cohorts. We evaluated the diagnostic utility of SNAP25 in plasma and CSF, as well as its associations with cognitive performance and imaging outcomes, such as amyloid PET and tau PET. In addition, we examined the relationship between SNAP25 levels and SV2A PET measures and compared these associations with those of neurofilament light (NfL), a marker commonly used to reflect axonal injury and neurodegeneration.

Materials and methods

Study design and population

BioFINDER pilot cohort: This cohort contains a selection of samples (*n* = 102, Table 1) from the BioFINDER-2 study (NCT03174938) [38]. The CU individuals were all required to be above the age of 65, as well as having a Mini-Mental State Examination (MMSE) score of above 26 at the screening visit. In addition, absence of cognitive symptoms assessed by a physician, and not fulfilling any criteria for MCI or any forms of dementia according to Diagnostic and Statistical Manual and Mental Disorders, fifth edition (DSM-5) was required [39].. The AD patients fulfilled the AD criteria stated in the DSM-5 [39], as well as being Aβ-positive (defined by using the CSF Aβ42/Aβ40 ratio, with a cutoff of < 0.752 determined by mixture modelling) as previously described [40]. Participants were further stratified into analytical groups based on cognitive status (CU or cognitively impaired [CI]) and CSF amyloid-β (Aβ) status (+/-). All participants were recruited at Skåne University Hospital between April 2017 and September 2019. Participants and/or their relatives provided written informed consent. Ethical approval was provided by the Regional Ethical Committee in Lund, Sweden (ethical approval no. 2016/1053). The study adhered to the guidelines outlined in the World Medical Association Declaration of Helsinki and the Department of Health and Human Services Belmont Report.

Table 1
Baseline characteristics of the different cohorts.

Group	BioFINDER Pilot			GMC					TRIAD			
	CU-	CI+	p.value	CU-	CU+	CI-	CI+	p.value	CU-	CI-	CI+	p.value
n	50	52	-	35	11	21	39	-	10	16	10	-
Age	77.7 ± 6.3	73.7 ± 7.4	0.004	64.0 ± 7.8	69.5 ± 8.3	67.5 ± 10.4	71.0 ± 6.7	0.004	68.5 ± 6.3	64.4 ± 8.9	72.1 ± 7.6	0.067
Sex	-	-	0.030	-	-	-	-	0.710	-	-	-	1.000
male	30	20	-	19	4	12	20	-	5	8	5	-
female	20	32	-	16	7	9	19	-	5	8	5	-
YOE	NA	NA	-	15.3 ± 3.4	16.7 ± 2.8	13.1 ± 3.8	14.1 ± 3.5	0.021	NA	NA	NA	-
MMSE	29.0 [29.0–30.0]	21.0 [16.0–23.5]	< 0.001	29.0 [28.0–30.0]	29.0 [28.0–30.0]	28.0 [26.5–29.0]	26.0 [23.0–27.0]	< 0.001	29.0 [29.0–30.0]	29.0 [28.5–30.0]	28.0 [28.0–29.0]	0.104
Aβ42/40 (CSF)	1.05 [0.97–1.13]	0.50 [0.43–0.56]	< 0.001	0.10 [0.09–0.10]	0.05 [0.05–0.06]	0.08 [0.08–0.09]	0.05 [0.04–0.06]	< 0.001	-	-	-	-
pTau181 (CSF)	38.0 [31.2–51.8]	82.0 [64.8–98.8]	< 0.001	227 [181–290]	544 [349–684]	222 [133–325]	758 [490–961]	< 0.001	-	-	-	-
tTau (CSF)	284 [229–360]	582 [480–822]	< 0.001	-	-	-	-	-	-	-	-	-
VAMP2 (CSF)	364 [291–503]	407 [311–588]	0.046	-	-	-	-	-	315 [302–455]	536 [460–794]	444 [338–603]	0.233
pTau217 (Plasma)	-	-	-	0.17 [0.14–0.17]	0.34 [0.34–0.34]	0.39 [0.39–0.39]	0.60 [0.39–0.97]	0.054	0.19 [0.14–0.28]	0.25 [0.20–0.32]	1.80 [1.28–2.31]	< 0.001
pTau231 (Plasma)	-	-	-	7.69 [4.21–10.0]	10.9 [9.88–11.8]	6.59 [6.59–6.59]	12.2 [8.89–16.1]	0.103	11.9 [8.83–13.8]	11.9 [9.38–15.6]	25.9 [22.9–32.5]	< 0.001
NFL (Plasma)	24.9 [19.2–30.4]	32.5 [25.9–39.6]	< 0.001	13.8 [10.5–16.2]	13.4 [12.8–13.9]	46.9 [46.9–46.9]	20.8 [16.5–25.7]	< 0.001	16.9 [13.4–20.2]	16.9 [12.0–19.2]	28.0 [24.6–37.1]	0.030
VAMP2 (Plasma)	20.0 [15.9–25.0]	22.8 [14.6–28.7]	0.809	-	-	-	-	-	25.1 [23.0–28.8]	19.6 [15.7–23.1]	20.8 [19.7–30.9]	0.215
Tau PET	1.17 [1.10–1.21]	2.04 [1.57–2.56]	< 0.001	1.14 [1.09–1.18]	1.42 [1.32–1.43]	1.19 [1.16–1.35]	1.37 [1.28–1.71]	0.017	0.85 [0.82–0.88]	0.81 [0.76–0.87]	1.62 [1.25–2.16]	< 0.001
Amyloid PET	0.93 [0.91–0.97]	1.59 [1.38–1.81]	< 0.001	0.87 [0.86–0.89]	1.20 [1.01–1.32]	0.87 [0.85–0.91]	1.29 [1.23–1.38]	< 0.001	1.27 [1.24–1.32]	1.25 [1.23–1.27]	2.83 [2.39–3.08]	< 0.001
SV2A PET	-	-	-	-	-	-	-	-	3.50 [3.25–3.62]	3.30 [2.97–3.55]	3.37 [3.27–3.57]	0.159

Note. Age and years of education are presented as mean ± standard deviation. MMSE and biomarker data are presented as median [interquartile range].

p-values for MMSE and biomarkers were obtained from ANCOVA models adjusted for age, sex, and years of education when available; biomarker values were log-transformed before analysis.

Age and years of education were compared across groups using one-way ANOVA.

Group	BioFINDER Pilot			GMC					TRIAD			
	CU-	CI+	p.value	CU-	CU+	CI-	CI+	p.value	CU-	CI-	CI+	p.value

Sex distribution was compared across groups using Pearson's χ^2 test, or Fisher's exact test when assumptions for the χ^2 test were violated.

Abbreviations: Aβ1-42/1-40, amyloid beta protein ratio 1-42/1-40; AD, Alzheimer's disease;

CSF, cerebrospinal fluid; CI, cognitively impaired; CU, cognitively unimpaired;

MCI, mild cognitive impairment; MMSE, Mini-Mental State Examination; NFL, neurofilament light;

pTau181, phosphorylated tau at amino acid Thr181; pTau217, phosphorylated tau at amino acid Thr217;

pTau231, phosphorylated tau at amino acid Thr231; PET, positron emission tomography;

SV2A, synaptic vesicle protein 2A; VAMP2, vesicle-associated membrane protein 2;

YOE, years of education.

The Geneva Memory Center cohort (GMC; Geneva University Hospitals, Geneva, Switzerland), validation cohort: Contains a selection of participants (*n* = 106, Table 1) from the ongoing memory clinic cohort. The cohort includes cognitively unimpaired volunteers, individuals with subjective cognitive decline (SCD), MCI, and dementia. Participants have undergone extensive clinical, neuropsychological evaluation, as well as biomarker and neuroimaging assessments.

For the present study, CSF samples were available for all 106 participants including healthy volunteers (*n* = 22), SCD (*n* = 24), MCI (*n* = 48), and dementia (*n* = 12). Plasma samples were available for a subset of these participants (*n* = 42), including volunteers (*n* = 20), SCD (*n* = 4), MCI (*n* = 14), and dementia (*n* = 4). Due to limited sample size in some diagnostic groups, participants were grouped into CU (healthy volunteers and SCD) and a CI group (MCI and dementia). These groups were further stratified based on Aβ pathology status (+/-) for statistical analyses. Amyloid positivity was determined using amyloid PET (^{18}F-flutemetamol) with a standardized uptake value ratio (SUVR) cutoff > 1.03 [41] when PET data were available. In the absence of amyloid PET data, amyloid status was determined using the CSF Aβ42/pTau ratio, with assay-specific cutoffs of < 14.3 for INNOTEST and < 16.4 for Lumipulse. Among participants with both measures available, PET and CSF amyloid pathology classification showed 91.3% concordance (73/80). All plasma participants had corresponding CSF samples available. The study was approved by the Geneva Ethics Committee (CCER_2020_00403) and is conducted in accordance with the Helsinki Declaration of 1975.

Translational Biomarkers of Aging and Dementia (TRIAD; McGill University, Montreal, Canada), validation cohort: Contains a selection of participants from the TRIAD cohort that had available plasma samples and had undergone SV2A PET (*n* = 36, Table 1). The cohort included CU individuals (*n* = 10), as well as participants diagnosed with MCI (*n* = 9), AD (*n* = 2), FTD (*n* = 7), primary progressive aphasia (*n* = 3), progressive supranuclear palsy (*n* = 2), vascular cognitive impairment (*n* = 2), or corticobasal syndrome (*n* = 1). Clinical diagnoses were established through comprehensive neurophysiological assessment [42], including MMSE, Clinical Dementia Rating (CDR), and the NIA-AA criteria. CU individuals showed no objective cognitive deficits, with MMSE scores ≥ 26 and CDR = 0. Individuals with MCI showed objective cognitive impairment, with MMSE scores ≥ 26 and CDR = 0.5. AD dementia cases met NIA-AA criteria for probable AD, as determined by a dementia specialist, had MMSE scores < 26 and CDR ≥ 0.5, and were Aβ positive. Non-AD cases comprised of dementia cases with suspected non-AD pathophysiology, confirmed by negative Aβ PET biomarkers, with CDR > 0.5. Diagnoses were established by a consensus of neurologists based on clinical presentation and brain images. The non-AD participants did not meet criteria for other neurological or neuropsychiatric disorders.

Participants were subsequently classified into three analytic groups for analysis, CU amyloid-negative (CU−), CI amyloid-negative (CI−), and CI amyloid-positive (CI+), based on cognitive status and amyloid PET SUVR.

All participants in the TRIAD study provided written informed consent, and ethical approval was obtained from both the Douglas Mental Health University Institute Research Ethics Board (MP-18-2017-157) and the Montreal Neurological Institute (MNI) PET working committee and was conducted in accordance with the Declaration of Helsinki.

SNAP25 analysis

BioFINDER pilot cohort: CSF samples were collected by lumbar puncture in polypropylene tubes and immediately centrifuged at 2200 × g at 20 ˚C for 10 min, before being stored at -80 ˚C. The core AD biomarkers ($A\beta_{1-42/1-40}$ ratio, neurofilament light (NfL), p-tau181, and t-tau, were analysed using the NeuroToolKit (Roche Diagnostics) on a Cobas e601 instrument. The matching plasma samples were collected using EDTA-treated tubes. After collection the plasma samples were centrifuged at 4000 × g at 20 ˚C for 10 min, the supernatant was then removed and the samples stored at -80 ˚C pending analysis.

GMC: CSF and plasma samples collection is described elsewhere [43]. Briefly CSF samples were collected at the GMC according to the institution's internal protocols. Samples were subsequently archived in the hospital's local biobank. CSF concentrations of Aβ42, Aβ40, p-tau181 and t-tau were determined using INNOTEST or LUMIPULSE immunoassays (Fujirebio, Ghent, Belgium) at a certified chemistry laboratory of Geneva University Hospitals, following the manufacturer's guidelines. Blood samples were drawn into EDTA tubes and left at room temperature for two hours prior to centrifugation at 1700 g for 15 minutes. Plasma was then aliquoted into 1.2 mL polypropylene tubes (500 µL per aliquot) and stored at − 80°C in the local biobank of the GMC.

TRIAD: CSF and plasma samples were collected as previously described [44]. Briefly, CSF was collected into polypropylene tubes then subsequently centrifuged at 20 ˚C for 10 min at 2200 × g, before rapidly frozen at -80 ˚C. Plasma was collected as previously described [45]. Briefly, plasma was drawn and immediately transferred into ethylenediaminetetraacetic acid (EDTA)-treated tubes before centrifuging for 10 min at 5000 × g. After centrifugation the samples were transferred to new tubes for storage at -80 ˚C pending analysis. All the CSF and plasma markers, NfL, GFAP, p-tau181, p-tau217, p-tau231, and vesicle-associated membrane protein 2 (VAMP2) were quantified with custom single molecule array (Simoa) assays [46–49] on an HD-X instrument (Quanterix, Billerica, MA).

SNAP25 was measured according to the developer's instructions [29] on the HD-X instrument (Quanterix). Briefly, SNAP25 was quantified in both plasma (diluted 1:6), and CSF (diluted 1:120), using a mouse monoclonal antibody (ADx404) targeting the N-terminal end of human SNAP25 as capture antibody, coupled to paramagnetic beads. Another biotinylated mouse monoclonal antibody (RD-086) was used as the detector. All samples were above the lower limit of quantification of 2.91 pg/mL. All individual runs were monitored using run validation (RV) and quality control (QC) samples and all runs were qualified using ranges defined prior to this clinical study (data not shown).

Neuroimaging data

In the BioFINDER pilot cohort, magnetic resonance imaging (MRI) data were acquired on a 3T Siemens MAGNETOM Prisma scanner (Siemens Medical Solutions) using a T1-weighted magnetization-prepared rapid gradient echo (MPRAGE) sequence with 1 mm isotropic resolution. PET imaging was performed on digital GE Discovery MI scanners. Participants underwent amyloid PET approximately 90–110 minutes following administration of ~ 185 MBq [^{18}F]flutemetamol and tau PET approximately 70–90 minutes after injection of ~ 370 MBq [^{18}F]RO948.

Image processing was carried out according to previously described procedures [50]. Briefly, PET scans were corrected for attenuation and motion, summed, and co-registered to the temporally closest T1-weighted MRI scan. Structural MRI data were processed using the FreeSurfer v6.0 longitudinal pipeline. SUVR images were generated using cerebellar grey matter as the reference region for [^{18}F]flutemetamol and inferior cerebellar grey matter for [^{18}F]RO948.

Global Aβ burden was quantified as the mean SUVR across a composite neocortical region including the prefrontal, lateral temporal, parietal, anterior cingulate, and posterior cingulate/precuneus cortices. Aβ PET positivity was defined by a SUVR threshold exceeding 1.03 [51]. Tau burden was assessed using a temporal meta-region of interest (meta-ROI) comprising the bilateral entorhinal cortex, amygdala, fusiform gyrus, parahippocampal cortex, and inferior and middle temporal cortices, with tau PET positivity defined by a previous established SUVR threshold exceeding 1.36 [52]. Neurodegeneration was assessed using mean cortical thickness within an AD-signature temporal ROI consisting of the bilateral entorhinal, fusiform, inferior temporal, and middle temporal cortices.

In the GMC cohort PET imaging was performed using ^{18}F-flutemetamol, ^{18}F-florbetapir, and ^{18}F-flortaucipir at the Nuclear Medicine and Molecular Imaging Division of Geneva University Hospitals, on either a Biograph mCT or Biograph Vision PET/CT scanner (Siemens Healthineers, Erlangen, Germany), following tracer-specific acquisition protocols. ^{18}F-florbetapir scans were initiated 50 minutes after intravenous injection of approximately 200 MBq and acquired over 15 minutes. ^{18}F-flutemetamol scans began 90 minutes after administration of approximately 150 MBq and were acquired over 20 minutes. ^{18}F-flortaucipir scans started 75 minutes

post-injection of 180 MBq and were acquired over 30 minutes. All images were reconstructed using a 3D ordered subset expectation maximization (OSEM) algorithm (4 iterations, 12 subsets on the Biograph mCT; 4 iterations, 5 subsets on the Biograph Vision), with corrections applied for randoms, dead time, normalization, scatter, attenuation, and sensitivity. All PET and MRI images were reoriented to the anterior commissure–posterior commissure line in MATLAB (version 2021a). Amyloid and tau PET images underwent the same preprocessing pipeline, developed in-house at the GMC [53]. Global amyloid burden was quantified using the mean SUVR across the following regions: anterior cingulate cortex, posterior cingulate cortex, lateral temporal cortex, precuneus, parietal, frontal cortex. Global tau load was assessed as the mean SUVR across four regions of interest: the parahippocampal gyrus, amygdala, mid-occipital cortex, and inferior temporal cortex.

In the TRIAD cohort, PET data were acquired on a Siemens High Resolution Research Tomograph (Siemens Medical Solutions, Knoxville, TN), as previously described [54]. Standard preprocessing included corrections for photon attenuation, head motion, radioactive decay, detector dead time, as well as scatter and random events. Each PET image was co-registered to the corresponding native T1-weighted MRI using linear registration and subsequently transformed into the MNI space via the MRI-derived normalization parameters. Spatial smoothing was applied to each image to achieve a final resolution of 8 mm full width at half maximum.

For Aβ imaging, ([18F]AZD4694) images were acquired 40–70 minutes after tracer administration. Global SUVR was computed using cerebellar grey matter as the reference region and average retention in the precuneus, cingulate cortex, inferior parietal lobule, medial prefrontal cortex, lateral temporal cortex, and orbitofrontal cortex. Aβ positivity was defined by an SUVR threshold exceeding 1.55 [55].

Tau PET images were obtained using ([18F]MK6240), 90–110 minutes after tracer administration. SUVRs were normalized to cerebellar grey matter and global tau PET load was computed from average tracer retention within a temporal meta-ROI, including the entorhinal cortex, amygdala, fusiform gyrus, and inferior and middle temporal cortices. Tau PET positivity was defined by a previously established SUVR threshold exceeding 1.24 [56].

SV2A PET ([18F]SynVesT-1) images were acquired at 90–110 minutes post-injection of the tracer and normalized to the centrum semiovale to generate SUVR images. A global estimation of SV2A binding was derived from a meta-ROI, defined as the average tracer retention in the precuneus, cingulate, inferior parietal, medial prefrontal, lateral temporal, and orbitofrontal cortices.

Data processing and statistical analysis

All statistical analyses were performed using R (version 4.5.1). Categorical variables in the cohort demographics were assessed using Pearson's chi-square test, or Fisher exact test if assumptions of the Pearson chi-square test were violated. Continuous variables were assessed using either Kruskal-Wallis test or analysis of covariance (ANCOVA). Unless otherwise specified, adjusted analyses included age, sex, and years of education (YOE, when available), as covariates. All biomarkers were naturally log-transformed and z-standardized prior to analyses. Group-wise comparisons for SNAP25 were also calculated using ANCOVA, with adjustment for multiple comparisons using Tukey's method. Differences in the magnitude of diagnostic group effects between plasma and CSF SNAP25 were assessed using linear mixed-effects models including a diagnosis × matrix (plasma and CSF) interaction, with participant ID included as random intercept to account for paired plasma and CSF measurements. A receiver operating characteristics (ROC) curve was calculated, providing the area under the curve (AUC), which was used to evaluate discriminatory powers for diagnostic performance of the biomarker. DeLong test was applied to statistically compare AUCs. Correlations between continuous variables were assessed using Spearman's rank correlation coefficient (r_s), and partial correlations were assessed using Spearman's rank correlation with covariate adjustment. Associations between continuous variables and clinical or imaging outcomes were evaluated using linear regression models, with outcomes standardized prior to analysis. Accordingly, regression coefficients for biomarkers estimate the effects per standard deviation change in corresponding biomarker levels. Wald tests were used to compare the strength of associations between fluid biomarkers. Voxelwise associations between SNAP-25 and SV2A-PET measures were assessed using linear regression models adjusted for age and sex. These models were corrected for multiple comparisons using random field theory (RFT; $p \leq 0.05$).

Results

SNAP25 in Plasma and CSF

Plasma and CSF levels of SNAP25 in the three independent cohorts can be found in Fig. 1. In the BioFINDER pilot cohort, SNAP25 was significantly higher in CI+ compared to CU − in both plasma (fold change (FC) = 1.46, 95% CI = 1.26–1.69, $p < 0.0001$) and CSF (FC = 1.30, 95% CI = 1.15–1.49, $p < 0.001$; Fig. 1A). However, the magnitude of the disease-associated change was not significantly different between plasma and CSF when tested using a diagnosis × matrix interaction in a linear mixed-effects model (β = -0.26, 95% CI = -0.76–0.25, $p = 0.33$). SNAP25 displayed a modest accuracy in discriminating CI+ from CU − in plasma (AUC = 0.78, 95% CI = 0.69–0.87), as well as in CSF (AUC = 0.7, 95% CI = 0.60–0.81; Fig. 1.D) with no differences between their power to discriminate these two groups (DeLong > 0.05). Despite similar diagnostic performance, there was no correlation between plasma and CSF SNAP25 (r_s = 0.13, 95% CI = -0.06–0.33, $p > 0.05$; Supplementary Fig. 1A and Supplementary Table S1). However, plasma SNAP25 did correlate to plasma VAMP2 (r_s = 0.40, 95% CI = 0.21–0.57, $p < 0.001$), and plasma NfL (r_s = 0.41, 95% CI = 0.21–0.58, $p < 0.0001$), whereas CSF SNAP25 correlated with CSF VAMP2 (r_s = 0.88, 95% CI = 0.82–0.92, $p < 0.0001$), CSF NfL (r_s = 0.47, 95% CI = 0.30–0.62, $p < 0.0001$), and CSF pTau181 (r_s = 0.79, 95% CI = 0.69–0.85, $p < 0.0001$). Full correlations between all markers can be found in Supplementary Fig. 1A and Supplementary Table S1.

In the GMC cohort, SNAP25 was significantly higher in CI+ compared to CU − in plasma (FC = 1.48, 95% CI = 1.22–1.78, $p < 0.0001$) but not in CSF (FC = 1.19, 95% CI = 0.93–1.52, $p > 0.05$; Fig. 1B). However, there was a significant difference between CI− compared to CI + in CSF (FC = 1.38, 95% CI = 1.06–1.80, $p < 0.01$). Although the overall diagnosis × matrix interaction in a linear mixed-effects model did not reach statistical significance (p = 0.08), the magnitude of the CI+-associated change was significantly different between plasma and CSF (β = -0.66, 95% CI = -1.28 – -0.06, $p < 0.05$), indicating a stronger disease-related effect in plasma than in CSF. SNAP25 in CSF showed poor discrimination across the groups compared to CU− (CU+: AUC = 0.68, 95% CI = 0.49–0.86, CI−: AUC = 0.62, 95% CI = 0.46–0.77, CI+: AUC = 0.68, 95% CI = 0.55–0.80, Fig. 1E). However, SNAP25 in plasma showed a good accuracy for discriminating CI + and CU− (AUC = 0.92, 95% CI = 0.84–1.00, Fig. 1E), with a significant difference in their discriminating power (DeLong < 0.0001). In the separate groups, plasma SNAP25 showed a significant difference between MCI and CU (FC = 1.51, 95% CI = 1.27–1.74, $P < 0.0001$) and MCI and SCD (FC = 1.38, 95% CI = 0.87–5.41, $p < 0.05$), shown in Supplementary Fig. 2, but there were no significant differences in CSF. As opposed to the BioFINDER Pilot cohort, in the GMC cohort, there was a modest significant correlation between CSF and plasma for SNAP25 (r_s = 0.48, 95% CI = 0.18–0.68, $p < 0.01$; Supplementary Fig. 1B and Supplementary Table S1). Furthermore, SNAP25 in plasma had a significant correlation with plasma NfL (r_s = 0.62, 95% CI = 0.39–0.79, $p < 0.0001$), and the plasma pTau markers (pTau181: r_s = 0.40, 95% CI = 0.04–0.69, $p < 0.05$, pTau217: r_s = 0.80, 95% CI = 0.41–0.98, $p < 0.01$, pTau231: r_s = 0.65, 95% CI = 0.39–0.80, $p < 0.0001$), and CSF SNAP25 with the CSF pTau markers (pTau181: r_s = 0.67, 95% CI = 0.69–0.85, $p < 0.0001$, pTau217: r_s = 0.54, 95% CI = 0.37–0.66, $p < 0.0001$, pTau231: r_s = 0.72, 95% CI = 0.61–0.82, $p < 0.0001$). All correlations can be found in the Supplementary Fig. 1B and Supplementary Table S1.

For the TRIAD cohort, only plasma SNAP25 showed significant differences between groups. The biggest difference was between CI + and CI− (FC = 2.07, 95% CI = 1.40–3.07, $P < 0.001$), followed by CI + and CU− (FC = 1.77, 95% CI = 1.18–2.66, $p < 0.01$; Fig. 1C). In this cohort, diagnostic effects were significantly different between plasma and CSF when tested jointly across diagnostic groups using a diagnosis × matrix interaction in a linear mixed-effects ($p < 0.05$). However, no individual diagnostic group showed a significant differential effect between plasma and CSF when examined separately. Regarding discriminating CU− from the other groups (Fig. 1F), SNAP25 showed the best discrimination in plasma for CI+ (AUC = 0.90, 95% CI = 0.76–1.00), with CI− having a weak discrimination (AUC = 0.83, 95% CI = 0.49–1.00). In CSF, CI− (AUC = 0.78, 95% CI = 0.49–1.00) had the strongest discrimination and CI + had a modest discrimination (AUC = 0.68, 95% CI = 0.37–0.98). However, the CSF groups are rather small, which affects the outcome of the AUC. Furthermore, there was no significant difference between plasma and CSF (DeLong p > 0.05). In the full TRIAD cohort, there was also a modest albeit not significant correlation for SNAP25 in plasma and CSF (r_s = 0.46, 95% CI = 0.03–0.74, $p = 0.08$; Supplementary Fig. 1C and Supplementary Table S1). SNAP25 in plasma was significantly correlated with plasma VAMP2 (r_s = 0.36, 95% CI = 0.03–0.63, $p < 0.05$), plasma NfL (r_s = 0.44, 95% CI = 0.16–0.67, $p < 0.01$), plasma pTau217 (r_s = 0.59, 95% CI = 0.37–0.76, $p < 0.001$), and plasma pTau231 (r_s = 0.42, 95% CI = 0.11–0.64, $p < 0.05$), while SNAP25 in CSF correlated with CSF VAMP2 (r_s = 0.93, 95% CI = 0.79–0.97, $p < 0.0001$) and pTau217(r_s = 0.60, 95% CI = 0.16–0.91, $p < 0.01$). Full correlations can be found in the Supplementary Fig. 1C and Supplementary Table S1.

Association of SNAP25 with cognition, cortical thickness, amyloid and tau PET

In the full BioFINDER Pilot cohort, SNAP25 was associated with MMSE score in both plasma (β = -0.32, SE = 0.09, *P* < 0.001) and CSF (β = -0.26, SE = 0.09, *p* < 0.01; Fig. 2A). However, no significant association was observed in individual diagnostic groups for plasma, while there was a significant association to CU − in CSF (β = -0.06, SE = 0.02, *p* < 0.01; Supplementary Fig. 3). There was also an association in the full cohort to cortical thickness in plasma (β = -0.30, SE = 0.10, *p* < 0.01) and CSF (β = -0.20, SE = 0.10, *p* < 0.05; Fig. 2A), with no significant association in the separate diagnostic groups for neither plasma nor CSF. Furthermore, SNAP25 was also significantly associated with tau PET and amyloid PET, in both CSF (tau PET: β = 0.21, SE = 0.09, *p* < 0.05; amyloid PET: β = 0.36, SE = 0.10, *p* < 0.001; Fig. 2A) and plasma (tau PET: β = 0.21, SE = 0.09, *p* < 0.05; Fig. 2A, amyloid PET: β = 0.32, SE = 0.11, *p* < 0.01; Fig. 2A), with no significant associations observed for the individual diagnostic groups (Supplementary Fig. 3). A formal comparison between the coefficients in plasma and CSF using a Wald test showed no significant difference between the two (*p* > 0.05).

For the GMC cohort, SNAP25 was associated with MMSE score in CSF (β = -0.23, SE = 0.10, *p* < 0.05, Fig. 2A), and showed the same trend in plasma, although it did not reach statistical significance (β = -0.32, SE = 0.18, *p* = 0.078, Fig. 2A). Furthermore, it was also associated with the clinical dementia rating (CDR) in plasma for the full cohort (β = 0.16, SE = 0.06, *p* < 0.01; Supplementary Fig. 4A), but not in CSF, or any individual diagnosis group. There was no association between SNAP25 and tau PET in this cohort. Regarding amyloid PET, there was a significant association between SNAP25 in CSF and amyloid PET both in the full cohort (β = 0.28, SE = 0.14, *p* < 0.05; Fig. 2A) and in the Volunteer- group (β = 0.34, SE = 0.16, *p* < 0.05; Supplementary Fig. 4B), but no association in plasma. Furthermore, SNAP25 in both plasma and CSF was also associated with lower brain volumes in multiple brain regions. In the full cohort, higher SNAP25 in plasma was associated with lower brain volumes in both the left (β = -0.35, SE = 0.13, *p* < 0.05; Supplementary Fig. 4A) and right (β = -0.31, SE = 0.14, *p* < 0.05; Supplementary Fig. 4A) thalamus, the left amygdala (β = -0.35, SE = 0.16, *p* < 0.05; Supplementary Fig. 4A), and the brain stem (β = -0.34, SE = 0.16, *p* < 0.05; Supplementary Fig. 4A), with no significant associations in the individual groups. For CSF, higher SNAP25 was associated with greater cortex volume (β = 0.21, SE = 0.09, *p* < 0.05; Supplementary Fig. 4A), and total grey volume (β = 0.20, SE = 0.09, *p* < 0.05; Supplementary Fig. 4A) in the full cohort. It was also associated with cortex volume in the CI− group (β = 0.34, SE = 0.16, *p* < 0.05, Supplementary Fig. 4B). Furthermore, higher CSF SNAP25 levels were also associated with lower ventricle volumes, in both the left (β = -0.40, SE = 0.09, *p* < 0.0001; Supplementary Fig. 4A) and the right (β = -0.42, SE = 0.08, *p* < 0.0001; Supplementary Fig. 4A) lateral ventricles, as well as the third ventricle (β = -0.37, SE = 0.07, *p* < 0.0001; Supplementary Fig. 4A), in the full cohort. This inverse association with ventricular volumes was also observed within both the CI− (left lateral ventricle: β = -0.37, SE = 0.15, *p* < 0.05; right lateral ventricle: β = -0.45, SE = 0.18, *p* < 0.05; third ventricle: β = -0.50, SE = 0.18, *p* < 0.05, Supplementary Fig. 4B) and CI+ (left lateral ventricle: β = -0.58, SE = 0.12, *p* < 0.0001; right lateral ventricle: β = -0.63, SE = 0.12, *p* < 0.0001; third ventricle: β = -0.58, SE = 0.11, *p* < 0.0001, Supplementary Fig. 4B). Like observed in the BioFINDER cohort, when performing a formal comparison between the coefficients in plasma and CSF using a Wald test, there was no significant difference between the fluids (*P* > 0.05).

In the full TRIAD cohort, neither CSF nor plasma SNAP25 concentrations were associated with MMSE score or tau PET. However, SNAP25 in plasma was significantly associated with Aβ PET (β = 0.61, SE = 0.14, *p* < 0.001; Fig. 2A), and CSF was significantly associated with intracranial volume (β = -0.36, SE = 0.15, *p* < 0.05; Supplementary Fig. 5). For the individual diagnostic groups, SNAP25 was only significantly associated with tau PET in CSF for the CI+ group (β = -1.11, SE = 0.26, *p* < 0.05; Supplementary Fig. 5). As with both the other cohorts, there was no significant difference comparing coefficients in plasma and CSF using a Wald test (*P* > 0.05).

Association of SNAP25 with SV2A PET

Finally, we tested whether a synaptic protein measured in the biofluids is reflective of synaptic density in the brain as indexed by PET. To assess the relationship between SNAP25 and synaptic density, associations to SV2A PET were examined in the TRIAD cohort. Plasma NfL was included as a comparator biomarker. First, we evaluated the association between the fluid biomarkers and the global SV2A PET meta-ROI. In the full cohort, SNAP25 was not significantly associated with SV2A PET meta-ROI in either plasma (β = 0.31, SE = 0.16, *p* = 0.06; Fig. 2A) or CSF (β = 0.16, SE = 0.17, *p* = 0.35; Fig. 2A). In addition, no significant association was observed for plasma NfL (β = -0.20, SE = 0.22, *p* = 0.36). However, a partial Spearman correlation adjusted for age and sex, showed a significant association between plasma SNAP25 and SV2A PET meta-ROI (r_s = 0.36, *p* = 0.04), whereas no significant correlation was observed for CSF SNAP25 (r_s = 0.20, *p* = 0.44) or plasma NfL (r_s = -0.24, *p* = 0.16). In the CI+ subgroup, both plasma and CSF SNAP25 showed a significant association (plasma: β = 0.81, SE = 0.17, *p* < 0.01; Supplementary Fig. 5; CSF: β = 0.74, SE = 0.18, *p* < 0.05; Supplementary Fig. 5), whereas, again, no significant association was found for plasma NfL (β = 0.03, SE = 0.67, *p* = 0.96). Consistent with these

findings, partial Spearman adjusted for age and sex showed a significant correlation for SNAP25 in both plasma (r_s = 0.74, p = 0.04) and CSF (r_s = 0.99, p < 0.01), while no significant partial correlation was observed for NfL in the CI+ group (r_s = -0.17, p = 0.69).

In the voxelwise analysis, linear regression was used to assess the association of plasma NfL and SNAP25 with SV2A PET in the full cohort as well as in the CU−, CI−, and CI+ subgroups. No significant associations were observed for plasma NfL in any group (data not shown). Similarly, plasma SNAP25 was not associated with SV2A PET in the full cohort or among amyloid-negative individuals. However, in the CI+ group, several clusters showed significant positive associations between SNAP25 in plasma and SV2A PET, most prominently in the ventromedial prefrontal cortex (t > 3.1, Fig. 2B).

Together, these analyses demonstrate convergent results across both regional and voxelwise approaches for SNAP25 in relation to SV2A PET.

Discussion

In this study, we examined CSF and plasma levels of SNAP25 across three independent, well-characterized clinical cohorts and evaluated their associations with cognition, multimodal biomarkers, including tau, Aβ, and SV2A PET as well as structural MRI measures. These analyses provide insight into the relationship between SNAP25, synaptic integrity, and neurodegenerative processes.

Our findings showed significantly higher levels of SNAP25 in both CSF and plasma in the CI+ group in both the BioFINDER pilot cohort and the GMC cohort. In contrast, in the TRIAD cohort, significant group differences were only observed in plasma, while CSF differences did not reach statistical significance, possibly due to the low number of observations in these CSF groups. However, even if the levels of SNAP25 appeared to be changed to a greater extent in plasma compared with CSF across cohorts, a formal comparison of plasma to CSF effects indicated significant differences only in the TRIAD cohort. This effect was seen to a lesser extent in the GMC cohort as well, where a significant difference was observed for the CI+ subgroup, but not in the full cohort. Furthermore, we observed that SNAP25 changed with Aβ pathology, *e.g.*, in the TRIAD cohort, only the Aβ-PET positive group had increased levels of plasma SNAP25. The non-significant changes in CSF could again be due to lack of power. This was also observed in the BioFINDER pilot cohort, as well as in the GMC cohort. These results align with previous studies on SNAP25 in CSF [13–15, 28] and in plasma [29], where higher levels of SNAP25 have been shown in the disease groups. However, previous studies on SNAP25 in plasma are limited, and some have reported insufficient sensitivity [28].

We observed that correlations between plasma and CSF SNAP25 had mixed results in the three cohorts. For the BioFINDER pilot cohort, no significant correlation was found, but modest significant correlations were found in both the GMC and TRIAD cohorts. These differences may reflect cohort-specific factors, including sample size, pre-analytical sample handling, as well as differences in disease-stage composition. Investigating SNAP25 correlation to other biomarkers, CSF SNAP25 correlated with both CSF tau markers (tTau, pTau181, pTau217, and pTau231) and CSF VAMP2, supporting its role as a proximal marker of synaptic pathology. A shared mechanistic SNARE pathway could also explain the rigorous correlation between CSF SNAP25 and CSF VAMP2 [57]. Furthermore, SNAP25 in plasma consistently correlated across the three cohorts to plasma NfL, a marker of axonal injury, plasma GFAP, marker for glial activation, as well as the pTau markers (pTau181, pTau217, and pTau231), which could reflect downstream neurodegenerative processes.

Associations between SNAP25 and multimodal markers varied between cohorts and clinical groups. SNAP25 showed an overall positive association with amyloid PET across the three independent cohorts, consistent with previous findings [58]. These results suggest that SNAP25 levels may reflect synaptic dysfunction associated with amyloid pathology, although the magnitude of these associations differed across the cohorts and biofluids. Significant associations with tau PET were observed in the BioFINDER cohort, as well as in the CI+ group in TRIAD. Together with the significant correlations between SNAP25 and the pTau and tTau markers, these findings suggest that SNAP25 reflects synaptic pathology occurring in the context of AD-related pathology, with associations observed for both amyloid and tau biomarkers. Associations between SNAP25 and cognition also differed across the cohorts. In the BioFINDER pilot cohort, SNAP25 was associated with MMSE score in both CSF and plasma. In the GMC cohort, a significant association with MMSE was observed for CSF SNAP25, while plasma SNAP25 showed a similar trend but did not reach statistical significance. In addition, plasma SNAP25 was associated with CDR in the full cohort, whereas no significant association with CDR was found for CSF SNAP25. For the TRIAD cohort, no significant association was observed. This variability between cohorts is

consistent with previous studies, which have reported inconsistent findings regarding the association between SNAP25 and cognitive measures [13, 14, 29], potentially reflecting differences in cohort compositions and disease stages.

While the biological function of SNAP25 is related to synaptic processes, its presence and subsequent increase in biofluids should not be assumed to be synapse-related. To investigate the relationship between SNAP25 and synaptic density we assessed its plasma and CSF associations with both meta-ROI and voxelwise SV2A PET. In the full TRIAD cohort, there was a trending albeit non-significant association between plasma SNAP25 and SV2A PET meta-ROI. However, we found a significant association between plasma SNAP25 and SV2A meta-ROI PET for the full cohort using a partial Spearman correlation, adjusted for age and sex, suggesting that a non-linear relationship might be present. Furthermore, in CI individuals with amyloid pathology present, both CSF and plasma SNAP25 showed a significant association to SV2A PET meta-ROI, across both regression and partial correlation analyses. There was also a significant association in this group for plasma SNAP25 and the voxelwise SV2A PET, most notably in the ventromedial prefrontal cortex. This was in contrast to NfL, a biomarker commonly used to reflect axonal injury, which did not show any significant association to either the regional meta-ROI PET or the voxelwise SV2A PET. These findings suggests that SNAP25 might relate more to synaptic density specifically in disease contexts where synaptic loss is established in an amyloid dependent manner, supporting its role as a marker of synaptic injury rather than a global measure of synaptic density.

This study was not without limitations. First, some subgroups had relatively small sample sizes which may account for some inconsistent findings between our three independent cohorts. SV2A PET data was only available in one out of the three cohorts, limiting the ability to replicate synaptic density associations across independent cohorts. Conversely, a key strength of this study is the use of multiple independent, well-characterized cohorts. All three cohorts included comprehensive amyloid and tau PET and MRI data, measurements of established biomarkers in both plasma and CSF, as well as clinical and cognitive assessment. This allowed for a detailed, cross-validated assessment of SNAP25 across different disease contexts.

Conclusions

Across three independent and well-characterized cohorts, we demonstrate that SNAP25 is reliably measurable in plasma, and those levels are consistently elevated in CI+ individuals. SNAP25 levels were associated with core AD biomarkers, including amyloid and tau measures, as well as structural and molecular imaging markers, supporting its relevance to AD-related synaptic pathology. Although associations with SV2A PET were modest in the overall sample, significant relationships were observed in amyloid-positive cognitively impaired individuals, suggesting that plasma SNAP25 may reflect synaptic injury particularly in the context of established AD. Together, these findings support plasma SNAP25 as a promising, minimally invasive biomarker of synaptic dysfunction that may be informative for disease characterization and for monitoring synaptic-integrity in interventions in clinical trials.

Declarations

Ethics approval and consent to participate

The BioFINDER-2 study was approved by the Regional Ethical Review Board in Lund, Sweden (ethical approval no. 2016/1053). The Geneva Memory Center study was approved by the Geneva Ethics Committee (CCER_2016-01346 and CCER_2020-00403). The TRIAD study was approved by the Douglas Mental Health University Institute Research Ethics Board (MP-18-2017-157) and the Montreal Neurological Institute PET Working Committee. All studies were conducted in accordance with the Declaration of Helsinki, and written informed consent was obtained from all participants before participation.

Data availability

BioFINDER pilot data will be made available to qualified academic investigators upon reasonable request for the purpose of reproducing the analyses and findings reported in this study, subject to applicable EU General Data Protection Regulation requirements, approval by the Swedish Ethical Review Authority and Region Skåne, and an appropriate data transfer agreement.

All requests for raw and analyzed data and materials will be promptly reviewed by McGill University to verify if the request is subject to any intellectual property or confidentiality obligations. Anonymized data will be shared upon request to the study's senior author from a qualified academic investigator for the sole purpose of replicating the procedures and results presented in this article. Any data and materials that can be shared will be released via a material transfer agreement. Data are not publicly available due to information that

could compromise the privacy of research participants. Related documents, including study protocol and informed consent forms, can similarly be made available upon request.

The data that support the findings of this study are available from the Principal Investigator, Prof. Giovanni B. Frisoni upon reasonable request. The data are not publicly available due to privacy and ethical restrictions regarding patient medical records.

Acknowledgements

HZ is a Wallenberg Scholar and a Distinguished Professor at the Swedish Research Council supported by grants from the Swedish Research Council (#2023-00356, #2022-01018 and #2019-02397), the European Union's Horizon Europe research and innovation programme under grant agreement No 101053962, Swedish State Support for Clinical Research (#ALFGBG-71320), the Alzheimer Drug Discovery Foundation (ADDF), USA (#201809-2016862), the AD Strategic Fund and the Alzheimer's Association (#ADSF-21-831376-C, #ADSF-21-831381-C, #ADSF-21-831377-C, and #ADSF-24-1284328-C), the European Partnership on Metrology, co-financed from the European Union's Horizon Europe Research and Innovation Programme and by the Participating States (NEuroBioStand, #22HLT07), the Bluefield Project, Cure Alzheimer's Fund, the Olav Thon Foundation, the Erling-Persson Family Foundation, Familjen Rönströms Stiftelse, Familjen Beiglers Stiftelse, Stiftelsen för Gamla Tjänarinnor, Hjärnfonden, Sweden (#FO2022-0270), the European Union's Horizon 2020 research and innovation programme under the Marie Skłodowska-Curie grant agreement No 860197 (MIRIADE), the European Union Joint Programme – Neurodegenerative Disease Research (JPND2021-00694), the National Institute for Health and Care Research University College London Hospitals Biomedical Research Centre, the UK Dementia Research Institute at UCL (UKDRI-1003), and an anonymous donor.

LSM is supported by grants from Anna-Lisa och Bror Björnsons Stiftelse, Herbert och krain jacobssons stiftelse (2025-Forskning-461), Gun och Bertil Stohnes Stiftelse (2025-034), Stiftelsen För Gamla Tjänarinnor (2025-365), and Adlerbert Research Foundation.

The TRIAD cohort study is supported by the Weston Brain Institute, Canadian Institutes of Health Research (CIHR) [MOP-11-51-31; RFN 152985, 159815, 162303], Canadian Consortium of Neurodegeneration and Aging (CCNA; MOP-11-51-31-team 1), Brain Canada Foundation (CFI Project 34874; 33397), the Fonds de Recherche du Québec – Santé (FRQS; 2020-VICO-279314; 2024 VICO-356138; https://doi.org/10.69777/324345 ; https://doi.org/10.69777/356138 and https://doi.org/10.69777/312994), and the Colin J Adair Charitable Foundation. P.R-N and SG are members of the CIHR-CCNA Canadian Consortium of Neurodegeneration in Aging.

Competing interests

HZ has served at scientific advisory boards and/or as a consultant for Abbvie, Acumen, Alamar, Alector, Alzinova, ALZpath, Amylyx, Annexon, Apellis, Artery Therapeutics, AZTherapies, Bioventix, Cognitact, Cognito Therapeutics, CogRx, Denali, Eisai, Enigma, Johnson & Johnson, LabCorp, Merck Sharp & Dohme, Merry Life, Nervgen, New Amsterdam, Novo Nordisk, Optoceutics, Passage Bio, Pinteon Therapeutics, Prothena, Quanterix, Red Abbey Labs, reMYND, Roche, Samumed, ScandiBio Therapeutics AB, Siemens Healthineers, Triplet Therapeutics, and Wave, has given lectures sponsored by Alzecure, BioArctic, Biogen, Cellectricon, Fujirebio, LabCorp, Lilly, Novo Nordisk, Oy Medix Biochemica AB, Roche, and WebMD, is a co-founder of Brain Biomarker Solutions in Gothenburg AB (BBS), which is a part of the GU Ventures Incubator Program, and is a shareholder of CERimmune Therapeutics (outside submitted work). OH is an employee of Eli Lilly. CDR, JG, and EV are employees of Fujirebio. All other authors report no conflicts of interest.

Funding

This work did not receive any specific grant from either public, commercial, or not-for-profit agencies. Fujirebio provided assay kits for measurements of SNAP25 in CSF and plasma, but had no role in study design, data collection, analysis and interpretation of data, or drafting of manuscript.

Authors' contributions

MS, NJA, PRN, HZ, and GV jointly developed the study and its design. LG, SJ, NR, AC, LT, and FR contributed to data collection. MS and LSM contributed with data analysis. LSM contributed with PET imaging analysis. MS drafted the manuscript, tables and figures. All authors reviewed the manuscript and approved the final version.

Consent for publication

Not applicable.

References

1. Selkoe DJ. Alzheimer's Disease Is a Synaptic Failure. Science. 2002;298(5594):789–91. 10.1126/science.1074069.
2. Gelon PA, Dutchak PA, Sephton CF. Synaptic dysfunction in ALS and FTD: anatomical and molecular changes provide insights into mechanisms of disease. Front Mol Neurosci. 2022;15:1000183. 10.3389/fnmol.2022.1000183 . PubMed PMID: 36263379; PubMed Central PMCID: PMC9575515.
3. Frigerio I, Bouwman MMA, Noordermeer RTGMM, Podobnik E, Popovic M, Timmermans E, et al. Regional differences in synaptic degeneration are linked to alpha-synuclein burden and axonal damage in Parkinson's disease and dementia with Lewy bodies. Acta Neuropathol Commun. 2024;12(1):4. 10.1186/s40478-023-01711-w.
4. Holmes SE, Honhar P, Tinaz S, Naganawa M, Hilmer AT, Gallezot JD, et al. Synaptic loss and its association with symptom severity in Parkinson's disease. Npj Park Dis. 2024;10(1):1–9. 10.1038/s41531-024-00655-9.
5. Osimo EF, Beck K, Reis Marques T, Howes OD. Synaptic loss in schizophrenia: a meta-analysis and systematic review of synaptic protein and mRNA measures. Mol Psychiatry. 2019;24(4):549–61. 10.1038/s41380-018-0041-5.
6. Kang HJ, Voleti B, Hajszan T, Rajkowska G, Stockmeier C, Licznerski P, et al. Decreased Expression of Synapse-Related Genes and Loss of Synapses in Major Depressive Disorder. Nat Med. 2012;18(9):1413–7. 10.1038/nm.2886 . PubMed PMID: 22885997; PubMed Central PMCID: PMC3491115.
7. Mecca AP, O'Dell RS, Sharp ES, Banks ER, Bartlett HH, Zhao W, et al. Synaptic density and cognitive performance in Alzheimer's disease: A PET imaging study with [^{11} C]UCB-J. Alzheimers Dement. 2022;18(12):2527–36. 10.1002/alz.12582.
8. Malpetti M, Jones PS, Cope TE, Holland N, Naessens M, Rouse MA, et al. Synaptic Loss in Frontotemporal Dementia Revealed by [C]UCB-J Positron Emission Tomography. Ann Neurol. 2023;93(1):142–54. 10.1002/ana.26543.
9. Bereczki E, Francis PT, Howlett D, Pereira JB, Höglund K, Bogstedt A, et al. Synaptic proteins predict cognitive decline in Alzheimer's disease and Lewy body dementia. Alzheimers Dement. 2016;12(11):1149–58. 10.1016/j.jalz.2016.04.005.
10. Südhof TC. Neurotransmitter release: the last millisecond in the life of a synaptic vesicle. Neuron. 2013;80(3):675–90.
11. Antonucci F, Corradini I, Fossati G, Tomasoni R, Menna E, Matteoli M. SNAP-25, a Known Presynaptic Protein with Emerging Postsynaptic Functions. Front Synaptic Neurosci. 2016;8:7. 10.3389/fnsyn.2016.00007 . PubMed PMID: 27047369; PubMed Central PMCID: PMC4805587.
12. Di Giovanni J, Iborra C, Maulet Y, Lévêque C, El Far O, Seagar M. Calcium-dependent Regulation of SNARE-mediated Membrane Fusion by Calmodulin*. J Biol Chem. 2010;285(31):23665–75. 10.1074/jbc.M109.096073.
13. Brinkmalm A, Brinkmalm G, Honer WG, Frölich L, Hausner L, Minthon L, et al. SNAP-25 is a promising novel cerebrospinal fluid biomarker for synapse degeneration in Alzheimer's disease. Mol Neurodegener. 2014;9:53. 10.1186/1750-1326-9-53 . PubMed PMID: 25418885; PubMed Central PMCID: PMC4253625.
14. Zhang H, Therriault J, Kang MS, Ng KP, Pascoal TA, Rosa-Neto P, et al. Cerebrospinal fluid synaptosomal-associated protein 25 is a key player in synaptic degeneration in mild cognitive impairment and Alzheimer's disease. Alzheimers Res Ther. 2018;10:80. 10.1186/s13195-018-0407-6 . PubMed PMID: 30115118; PubMed Central PMCID: PMC6097333.
15. Öhrfelt A, Brinkmalm A, Dumurgier J, Zetterberg H, Bouaziz-Amar E, Hugon J et al. A Novel ELISA for the Measurement of Cerebrospinal Fluid SNAP-25 in Patients with Alzheimer's Disease. Neuroscience. 2019;SNARE Proteins: A Long Journey of Science in Brain Health and Disease420:136–44. 10.1016/j.neuroscience.2018.11.038
16. Milà-Alomà M, Brinkmalm A, Ashton NJ, Kvartsberg H, Shekari M, Operto G, et al. CSF Synaptic Biomarkers in the Preclinical Stage of Alzheimer Disease and Their Association With MRI and PET. Neurology. 2021;97(21):e2065–78. 10.1212/WNL.0000000000012853 . PubMed PMID: 34556565; PubMed Central PMCID: PMC8610620.
17. Pereira JB, Janelidze S, Ossenkoppele R, Kvartsberg H, Brinkmalm A, Mattsson-Carlgren N, et al. Untangling the association of amyloid-β and tau with synaptic and axonal loss in Alzheimer's disease. Brain. 2020;144(1):310–24. 10.1093/brain/awaa395 . PubMed PMID: 33279949; PubMed Central PMCID: PMC8210638.
18. Clarke MTM, Brinkmalm A, Foiani MS, Woollacott IOC, Heller C, Heslegrave A, et al. CSF synaptic protein concentrations are raised in those with atypical Alzheimer's disease but not frontotemporal dementia. Alzheimers Res Ther. 2019;11(1):105. 10.1186/s13195-019-0564-2.
19. Das S, van Engelen MPE, Goossens J, Jacobs D, Bongers B, Fieldhouse JLP, et al. The use of synaptic biomarkers in cerebrospinal fluid to differentiate behavioral variant of frontotemporal dementia from primary psychiatric disorders and Alzheimer's disease.

Alzheimers Res Ther. 2024;16(1):34. 10.1186/s13195-024-01409-8.

20. Sandelius Å, Portelius E, Källén Å, Zetterberg H, Rot U, Olsson B, et al. Elevated CSF GAP-43 is Alzheimer's disease specific and associated with tau and amyloid pathology. Alzheimers Dement J Alzheimers Assoc. 2019;15(1):55–64. .006 PubMed PMID: 30321501; PubMed Central PMCID: PMC6333489.
21. De Vos A, Jacobs D, Struyfs H, Fransen E, Andersson K, Portelius E, et al. C-terminal neurogranin is increased in cerebrospinal fluid but unchanged in plasma in Alzheimer's disease. Alzheimers Dement. 2015;11(12):1461–9. 10.1016/j.jalz.2015.05.012.
22. Kvartsberg H, Portelius E, Andreasson U, Brinkmalm G, Hellwig K, Lelental N, et al. Characterization of the postsynaptic protein neurogranin in paired cerebrospinal fluid and plasma samples from Alzheimer's disease patients and healthy controls. Alzheimers Res Ther. 2015;7(1):40. 10.1186/s13195-015-0124-3 . PubMed PMID: 26136856; PubMed Central PMCID: PMC4487851.
23. Sauer M, Gomes BF, Shahrouki P, Lantero-Rodriguez J, Montoliu-Gaya L, Camporesi E, et al. Development and validation of a novel Simoa assay for NPTX2 in Alzheimer's disease and Down syndrome. Alzheimers Dement. 2025;21(6):e70241. 10.1002/alz.70241.
24. Oeckl P, Halbgebauer S, Anderl-Straub S, von Arnim CAF, Diehl-Schmid J, Froelich L, et al. Targeted Mass Spectrometry Suggests Beta-Synuclein as Synaptic Blood Marker in Alzheimer's Disease. J Proteome Res. 2020;19(3):1310–8. 10.1021/acs.jproteome.9b00824.
25. Chong JR, Ashton NJ, Karikari TK, Tanaka T, Schöll M, Zetterberg H, et al. Blood-based high sensitivity measurements of beta-amyloid and phosphorylated tau as biomarkers of Alzheimer's disease: a focused review on recent advances. J Neurol Neurosurg Psychiatry. 2021;92(11):1231–41. 10.1136/jnnp-2021-327370 . PubMed PMID: 34510001.
26. Das S, Goossens J, Jacobs D, Dewit N, Pijnenburg YAL et al. In 't Veld SGJG,. Synaptic biomarkers in the cerebrospinal fluid associate differentially with classical neuronal biomarkers in patients with Alzheimer's disease and frontotemporal dementia. Alzheimers Res Ther. 2023;15:62. 10.1186/s13195-023-01212-x PubMed PMID: 36964594; PubMed Central PMCID: PMC10037899.
27. Halbgebauer S, Abu-Rumeileh S, Oeckl P, Steinacker P, Roselli F, Wiesner D, et al. Blood β-Synuclein and Neurofilament Light Chain During the Course of Prion Disease. Neurology. 2022;98(14). 10.1212/WNL.0000000000200002.
28. Nilsson J, Ashton NJ, Benedet AL, Montoliu-Gaya L, Gobom J, Pascoal TA, et al. Quantification of SNAP-25 with mass spectrometry and Simoa: a method comparison in Alzheimer's disease. Alzheimers Res Ther. 2022;14(1):78. 10.1186/s13195-022-01021-8.
29. Gaetani L, Bellomo G, Chiasserini D, De Rocker C, Goossens J, Paolini Paoletti F, et al. Influence of co-pathology on CSF and plasma synaptic markers SNAP25 and VAMP2 in Alzheimer's disease and Parkinson's disease. Alzheimers Res Ther. 2025;17(1):115. 10.1186/s13195-025-01762-2.
30. Yao J, Nowack A, Kensel-Hammes P, Gardner RG, Bajjalieh SM. Cotrafficking of SV2 and Synaptotagmin at the Synapse. J Neurosci. 2010;30(16):5569–78. 10.1523/JNEUROSCI.4781-09. 2010 PubMed PMID: 20410110.
31. Bajjalieh SM, Peterson K, Linial M, Scheller RH. Brain contains two forms of synaptic vesicle protein 2. Proc Natl Acad Sci. 1993;90(6):2150–4. 10.1073/pnas.90.6.2150.
32. Bajjalieh M, Fran D, Weimann M, McConnell K. Differential Expression of Synaptic Vesicle Protein 2 (SV2) Isoforms. J Neurosci.
33. Janz R, Südhof TC. SV2C is a synaptic vesicle protein with an unusually restricted localization: anatomy of a synaptic vesicle protein family. Neuroscience. 1999;94(4):1279–90. 10.1016/S0306-4522(99)00370-X.
34. Nabulsi NB, Mercier J, Holden D, Carré S, Najafzadeh S, Vandergeten MC, et al. Synthesis and Preclinical Evaluation of 11C-UCB-J as a PET Tracer for Imaging the Synaptic Vesicle Glycoprotein 2A in the Brain. J Nucl Med. 2016;57(5):777–84. 10.2967/jnumed.115. .168179 PubMed PMID: 26848175.
35. Mecca AP, O'Dell RS, Sharp ES, Banks ER, Bartlett HH, Zhao W, et al. Synaptic density and cognitive performance in Alzheimer's disease: A PET imaging study with [11C]UCB-J. Alzheimers Dement. 2022;18(12):2527–36. 10.1002/alz.12582 . PubMed PMID: 35174954; PubMed Central PMCID: PMC9381645.
36. Coomans EM, Schoonhoven DN, Tuncel H, Verfaillie SCJ, Wolters EE, Boellaard R, et al. In vivo tau pathology is associated with synaptic loss and altered synaptic function. Alzheimers Res Ther. 2021;13:35. 10.1186/s13195-021-00772-0 . PubMed PMID: 33546722; PubMed Central PMCID: PMC7866464.

37. Vanderlinden G, Ceccarini J, Vande Casteele T, Michiels L, Lemmens R, Triau E, et al. Spatial decrease of synaptic density in amnestic mild cognitive impairment follows the tau build-up pattern. Mol Psychiatry. 2022;27(10):4244–51. 10.1038/s41380-022-01672-x.
38. BioFINDER [Internet]. [cited 2025 Oct 28]. The Swedish BioFINDER study. Available from: https://biofinder.se/
39. Diagnostic. and statistical manual of mental disorders: DSM-5. 5th ed. Washington: American psychiatric association; 2013.
40. Palmqvist S, Janelidze S, Quiroz YT, Zetterberg H, Lopera F, Stomrud E, et al. Discriminative Accuracy of Plasma Phospho-tau217 for Alzheimer Disease vs Other Neurodegenerative Disorders. JAMA. 2020;324(8):1–11. 10.1001/jama.2020.12134 . PubMed PMID: 32722745; PubMed Central PMCID: PMC7388060.
41. Quattrini G, Gatti E, Peretti DE, Aiello M, Chevalier C, Lathuiliere A, et al. [18F]flutemetamol uptake in the colon of a memory clinic population and its association with brain amyloidosis and the gut microbiota profile: an exploratory study. Eur J Nucl Med Mol Imaging. 2025;52(12):4591–603. 10.1007/s00259-025-07299-8 . PubMed PMID: 40314812; PubMed Central PMCID: PMC12491377.
42. Pascoal TA, Benedet AL, Tudorascu DL, Therriault J, Mathotaarachchi S, Savard M, et al. Longitudinal 18F-MK-6240 tau tangles accumulation follows Braak stages. Brain. 2021;144(11):3517–28. 10.1093/brain/awab248 . PubMed PMID: 34515754; PubMed Central PMCID: PMC8677534.
43. Ribaldi F, Chicherio C, Altomare D, Martins M, Tomczyk S, Jelescu I, et al. Brain connectivity and metacognition in persons with subjective cognitive decline (COSCODE): rationale and study design. Alzheimers Res Ther. 2021;13:105. 10.1186/s13195-021-00846-z . PubMed PMID: 34034799; PubMed Central PMCID: PMC8152092.
44. Therriault J, Pascoal TA, Lussier FZ, Tissot C, Chamoun M, Bezgin G, et al. Biomarker modeling of Alzheimer's disease using PET-based Braak staging. Nat Aging. 2022;2(6):526–35. 10.1038/s43587-022-00204-0.
45. Blood. phosphorylated tau 181 as a biomarker for Alzheimer's disease: a diagnostic performance and prediction modelling study using data from four prospective cohorts. Lancet Neurol. 2020;19(5):422–33. 10.1016/S1474-4422(20)30071-5
46. Gisslén M, Price RW, Andreasson U, Norgren N, Nilsson S, Hagberg L, et al. Plasma Concentration of the Neurofilament Light Protein (NFL) is a Biomarker of CNS Injury in HIV Infection: A Cross-Sectional Study. EBioMedicine. 2015;3:135–40. PubMed PMID: 26870824; PubMed Central PMCID: PMC4739412.
47. Suárez-Calvet M, Karikari TK, Ashton NJ, Lantero Rodríguez J, Milà-Alomà M, Gispert JD, et al. Novel tau biomarkers phosphorylated at T181, T217 or T231 rise in the initial stages of the preclinical Alzheimer's continuum when only subtle changes in Aβ pathology are detected. EMBO Mol Med. 2020;12(12):e12921. 10.15252/emmm.202012921 . PubMed PMID: 33169916; PubMed Central PMCID: PMC7721364.
48. Ashton NJ, Pascoal TA, Karikari TK, Benedet AL, Lantero-Rodriguez J, Brinkmalm G, et al. Plasma p-tau231: a new biomarker for incipient Alzheimer's disease pathology. Acta Neuropathol (Berl). 2021;141(5):709–24. 10.1007/s00401-021-02275-6 . PubMed PMID: 33585983; PubMed Central PMCID: PMC8043944.
49. Goossens J, Cervantes González A, Dewit N, Lidón L, Fortea J, Alcolea D, et al. Evaluation of cerebrospinal fluid levels of synaptic vesicle protein, VAMP-2, across the sporadic Alzheimer's disease continuum. Alzheimers Res Ther. 2023;15:186. 10.1186/s13195-023-01336-0 . PubMed PMID: 37898760; PubMed Central PMCID: PMC10612328.
50. Groot C, Smith R, Stomrud E, Binette AP, Leuzy A, Wuestefeld A, et al. Phospho-tau with subthreshold tau-PET predicts increased tau accumulation rates in amyloid-positive individuals. Brain. 2022;146(4):1580–91. 10.1093/brain/awac329 . PubMed PMID: 36084009; PubMed Central PMCID: PMC10115173.
51. Ossenkoppele R, Pichet Binette A, Groot C, Smith R, Strandberg O, Palmqvist S, et al. Amyloid and tau PET-positive cognitively unimpaired individuals are at high risk for future cognitive decline. Nat Med. 2022;28(11):2381–7. 10.1038/s41591-022-02049-x . PubMed PMID: 36357681; PubMed Central PMCID: PMC9671808.
52. Leuzy A, Smith R, Ossenkoppele R, Santillo A, Borroni E, Klein G, et al. Diagnostic Performance of RO948 F 18 Tau Positron Emission Tomography in the Differentiation of Alzheimer Disease From Other Neurodegenerative Disorders. JAMA Neurol. 2020;77(8):1–12. 10.1001/jamaneurol.2020.0989 . PubMed PMID: 32391858; PubMed Central PMCID: PMC7215644.
53. Dodich A, Mendes A, Assal F, Chicherio C, Rakotomiaramanana B, Andryszak P, et al. The A/T/N model applied through imaging biomarkers in a memory clinic. Eur J Nucl Med Mol Imaging. 2020;47(2):247–55. 10.1007/s00259-019-04536-9.
54. Macedo AC, Therriault J, Tissot C, Aumont É, Servaes S, Rahmouni N, et al. Modeling the progression of neuropsychiatric symptoms in Alzheimer's disease with PET-based Braak staging. Neurobiol Aging. 2024;144:127–37.

10.1016/j.neurobiolaging.2024.09.009.

55. Therriault J, Benedet AL, Pascoal TA, Savard M, Ashton NJ, Chamoun M, et al. Determining Amyloid-β Positivity Using 18F-AZD4694 PET Imaging. J Nucl Med Off Publ Soc Nucl Med. 2021;62(2):247–52. 10.2967/jnumed.120.245209 . PubMed PMID: 32737243.
56. Therriault J, Pascoal TA, Benedet AL, Tissot C, Savard M, Chamoun M, et al. Frequency of Biologically Defined Alzheimer Disease in Relation to Age, Sex, APOE ε4, and Cognitive Impairment. Neurology. 2021;96(7):e975–85. 10.1212/WNL.0000000000011416 . PubMed PMID: 33443136; PubMed Central PMCID: PMC8055338.
57. Wang C, Tu J, Zhang S, Cai B, Liu Z, Hou S, et al. Different regions of synaptic vesicle membrane regulate VAMP2 conformation for the SNARE assembly. Nat Commun. 2020;11:1531. 10.1038/s41467-020-15270-4 . PubMed PMID: 32210233; PubMed Central PMCID: PMC7093461.
58. Nilsson J, Pichet Binette A, Palmqvist S, Brum WS, Janelidze S, Ashton NJ, et al. Cerebrospinal fluid biomarker panel for synaptic dysfunction in a broad spectrum of neurodegenerative diseases. Brain. 2024;awae032. 10.1093/brain/awae032.

Figures

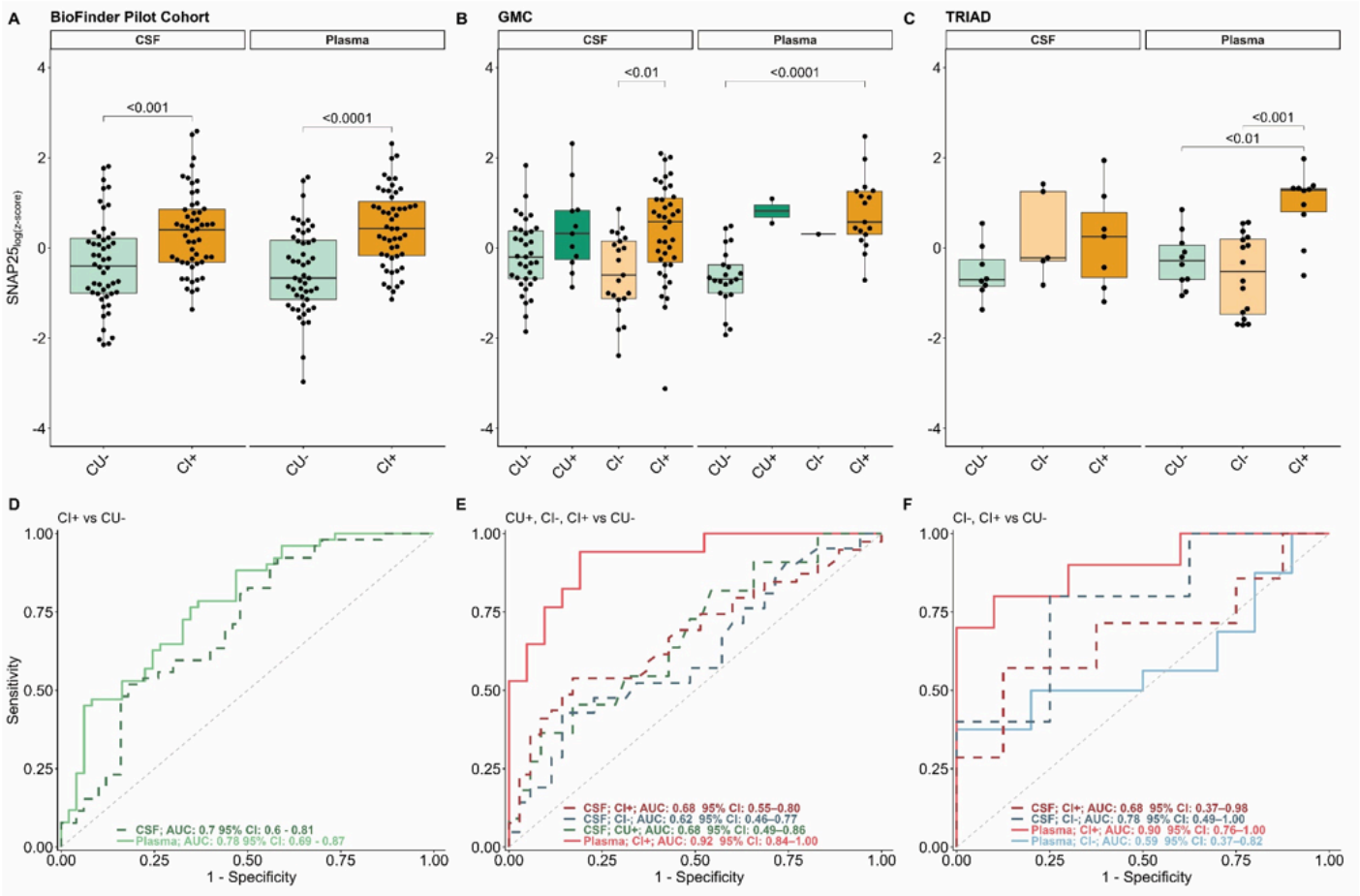


Figure 1

Biomarker group-wise comparison. (**A-C**) CSF and plasma levels of SNAP25, (**A**) BioFINDER Pilot Cohort: CU− (CSF: n = 50, Plasma: n = 50) and CI+ (CSF: n = 52, Plasma: n = 52). (**B**) GMC cohort: CU− (CSF: n = 35, Plasma: n = 21), CU+ (CSF: n = 11, Plasma: n = 2), CI− (CSF: n = 21, Plasma: n = 1), CI+ (CSF: n = 39, Plasma: n = 17). (**C**) TRIAD cohort: CU− (CSF: n = 8, Plasma: n = 10), CI− (CSF: n = 5, Plasma: n = 16), CI+ (CSF: n = 7, Plasma: n = 10). (**D-F**) ROC curves for SNAP25 in CSF and plasma, (**D**) BioFINDER Pilot Cohort: CI+ compared to CU−. (**E**) GMC cohort: CU+, CI−, and CI+ compared to CU−. (**F**) TRIAD cohort: CI−, and CI+ compared to CU−. Minus (−) and plus (+) denote Aβ-negative and Aβ-positive status, respectively. Boxplot p-values were obtained from a linear model adjusted for age, sex, and education when available. Horizontal line within boxplots denotes group median value, top and bottom of boxplots

denotes the 25th and 75th percentiles, whiskers show 1.5x interquartile range. AUC, area under the receiver operating characteristic curve; CSF, cerebrospinal fluid; CU, cognitively unimpaired; CI, cognitively impaired;

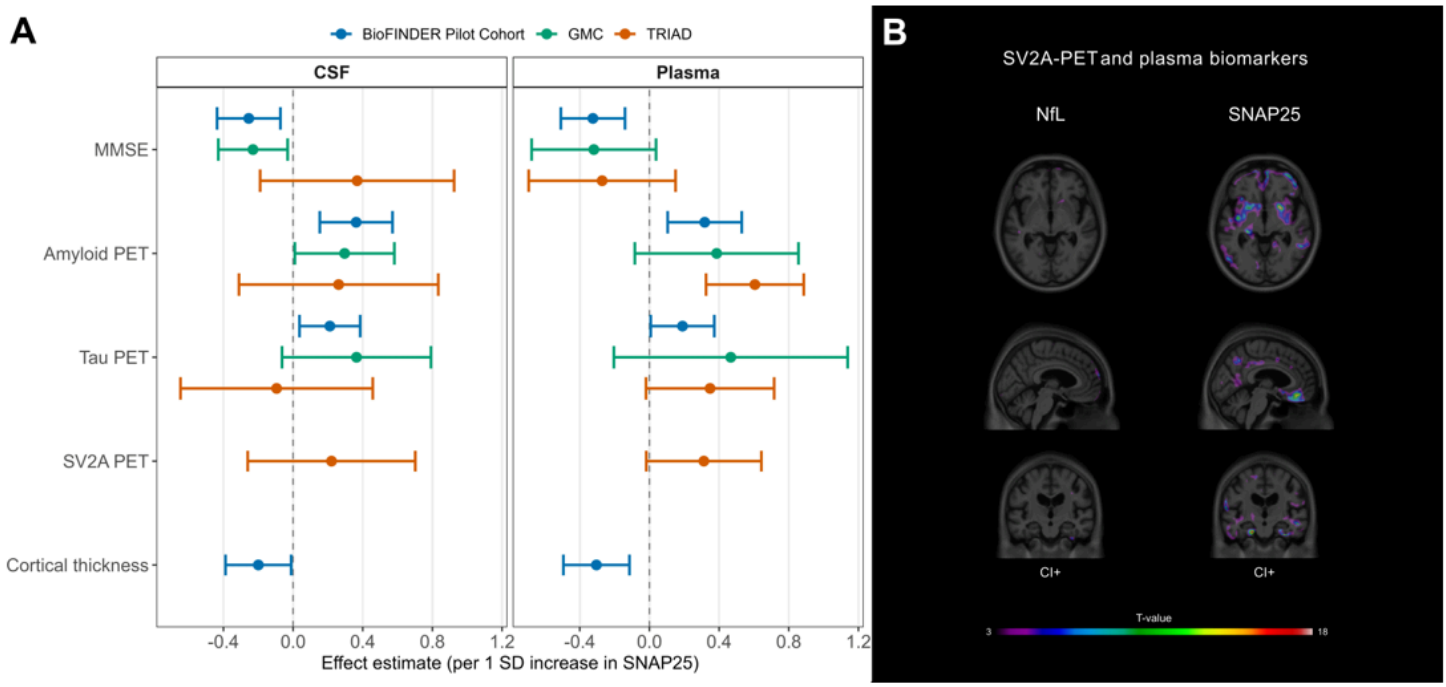


Figure 2

Associations between SNAP25 and cognitive, PET, and MRI measures. (**A**) Forest plots showing standardized effect estimates (β) and 95% confidence intervals for associations between SNAP25 and cognitive performance (MMSE), amyloid PET, tau PET, SV2A PET, and cortical atrophy. Associations are shown separately for CSF SNAP25 (left) and plasma SNAP25 (right) in the BioFINDER Pilot Cohort (blue), GMC (green), and TRIAD (orange). Linear regressions models were adjusted for age, sex, and education when available. Both SNAP25 concentrations and outcome measures were standardized (z-scored) prior to modelling, effect estimates therefore represent the change in outcome standard deviation per 1 SD increase in SNAP25. Error bars indicate 95% confidence intervals. (**B**) Voxelwise associations between plasma NfL or SNAP25 levels and SV2A PET in the CI+ subgroup of TRIAD. Models were corrected for multiple comparisons using RFT. Statistical maps are thresholded at t > 3.1, and displayed in axial, sagittal and coronal view. CI, cognitively impaired; CSF, cerebrospinal fluid; PET, positron emission tomography; SD, standard deviation

Supplementary Files

This is a list of supplementary files associated with this preprint. Click to download.

- SupplementaryTable1.docx
- SupplementaryFigures.docx